

## COSMIC DUST SYNTHESIS BY ACCRETION AND COAGULATION

G. PRABURAM<sup>1</sup> AND J. GOREE<sup>2</sup>

Department of Physics and Astronomy, University of Iowa, Iowa City, IA 52242

Received 1994 May 4; accepted 1994 September 21

### ABSTRACT

The morphology of grains grown by accretion and coagulation is revealed by a new laboratory method of synthesizing cosmic dust analogs. Submicron carbon particles, grown by accretion of carbon atoms from a gas, have a spherical shape with a cauliflower-like surface and an internal micro-structure of radial columns. This shape is probably common for grains grown by accretion at a temperature well below the melting point. Coagulated grains, consisting of spheres that collided to form irregular strings, were also synthesized. Another shape we produced had a bumpy non-spherical morphology, like an interplanetary particle collected in the terrestrial stratosphere. Besides these isolated grains, large spongy aggregates of nanometer-size particles were also found for various experimental conditions. Grains were synthesized using ions to sputter a solid target, producing an atomic vapor at a low temperature. The ions were provided by a plasma, which also provided electrostatic levitation of the grains during their growth. The temporal development of grain growth was studied by extinguishing the plasma after various intervals.

*Subject headings:* dust, extinction — plasmas — solar system: formation

### 1. INTRODUCTION

Dust is ubiquitous in space, including diffuse and dense interstellar media, circumstellar shells, dark interiors of molecular clouds, envelopes, nova ejecta, the outflow of red giant stars, and accretion disks (Cassinelli 1979; Woolf & Ney 1969; Lattimer 1982). Dust is an essential component of protoplanetary disks (O'Dell & Wen 1994), and its remnants are found widely in our solar system, including planetary rings, comet tails, and interplanetary space (Northrop & Hill 1983; Goertz 1989).

Much of what is known about cosmic dust has been learned from spectroscopy, including scattering, extinction, and emission. This requires fitting astrophysical observations to scattering theory, which in turn requires data that often can only be produced in laboratory experiments. Laboratory experiments are also useful because an electron microscope can yield images of grains grown under various conditions. This is valuable because the only cosmic grains that can be collected are interplanetary particles gathered by aircraft in the terrestrial stratosphere (Hill & Mendis 1979) and interstellar grains embedded in meteorites (Bernatowicz et al. 1991). Besides, in the laboratory it is possible to observe grains during their growth by accretion (grain-molecule collisions) and coagulation (grain-grain collisions).

In this paper we present images of carbon dust grains that we synthesized at a low temperature in the laboratory. These images offer useful insights into growth mechanisms and grain morphology for interplanetary and interstellar grains. We used a new method of synthesizing cosmic dust grain analogs. A flux of energetic ions sputters a target, releasing a physical vapor that can condense. A low-pressure plasma discharge is used to produce the ions and to charge and levitate dust grains, so that they remain suspended in the plasma, where they are exposed to the physical vapor, for minutes or hours.

The conditions in the protoplanetary disk that yielded our solar system are simulated in our process, including the tem-

perature and the gas number density. Grains grow by accretion and by coagulation, in our process as in the protoplanetary disk (Chokshi, Tielens, & Hollenbach 1993).

Besides its usefulness for synthesizing cosmic dust, our method also provides a simulation of dusty plasmas in space. In a plasma environment such as interstellar clouds, grains become electrically charged due to photoemission or absorption of electrons and ions. In theories of stellar formation it is proposed that charged grains provide an enhanced dissipation of a nebula's magnetic field, allowing MHD processes that limit the collapse to proceed faster (Nishi, Nakano, & Umebayashi 1991). The spokes in Saturn's rings arise so quickly that they can be explained only by attributing them to charged dust in the magnetospheric plasma (Goertz 1989). Finally, it has been proposed that intergrain electric potentials regulate the rate of grain coagulation in the early stages of planetary formation (Horanyi & Goertz 1990).

In the experiment reported here, we sputtered solid graphite targets and grew carbon grains. Spheroidal particles grew by accretion, and they have a cauliflower-like surface. Under certain growth conditions these spheroids coagulated, forming a mass of spheres pressed together in an irregular stringlike shape.

### 2. PRINCIPLES OF DUST GROWTH

In general, grain growth from the gas phase begins with nucleation, i.e., a cluster the size of a large molecule that forms from the gas. After this step, grains grow by two physical processes, accretion and coagulation, as sketched in Figure 1. Accretion leads to spherical or spheroidal particles, while coagulation can yield a shape that is nonspherical and often fractal (Weitz & Oliveria 1984). Coagulation can be followed by further growth by accretion, a step that has apparently not been stressed in the literature for cosmic grain growth, but is apparent in the experimental results presented in this paper.

In interstellar space and nebulae, grain growth must compete with several grain destruction processes. Radiation damage (by UV photons, electrons, protons,  $\alpha$ -particles, and heavier ions) can destroy grains by photodesorption, sputter-

<sup>1</sup> praburam@iowa.physics.uiowa.edu.

<sup>2</sup> john-goree@uiowa.edu.

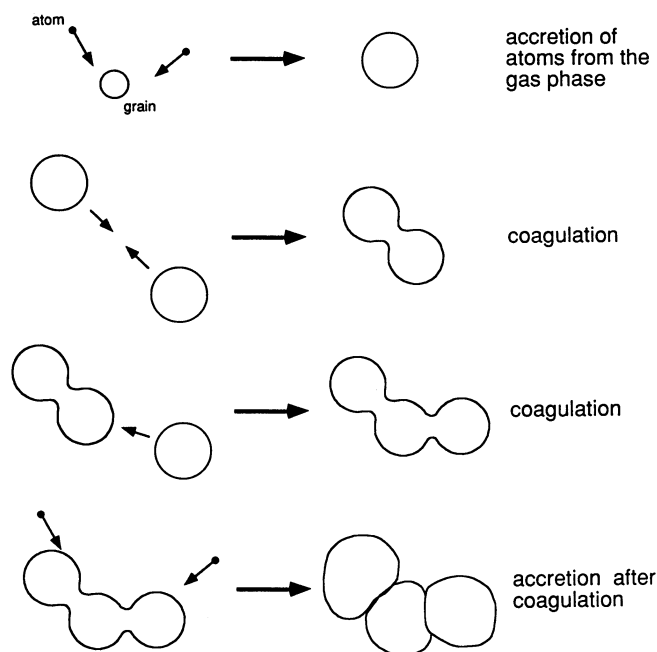


FIG. 1.—Grain growth processes. After an initial step of nucleation, grains can grow by accretion of atoms or by coagulation.

ing, and sublimation (Wehner, Kenknight, & Rosenberg 1963; Draine & Salpeter 1979; Johnson & Lanzerotti 1986; Seab & Shull 1983). Additional erosion can arise from grain-grain collisions, explosion of gas pockets, and separation of loosely connected grains (Northrop & Hill 1983). To the extent that these damage processes are selective in the types of grains they eliminate, they help determine the composition and size of interstellar grains.

Coagulation is recognized as an important grain growth process in the interstellar medium, as well as circumstellar, circumplanetary, and cometary environments. It is also believed that coagulation plays a critical role in planetary formation. Before planets can grow from collisions between planetesimals (Wetherill 1978) the planetesimals themselves must grow from interstellar grains and condensates of the solar nebula gas. The timescales of the sedimentation of large grains in an accretion disk and the subsequent formation of planetesimals are thought to be regulated by coagulation. Rapid sedimentation of big grains requires grain growth by coagulation, according to Mizuno, Markiewicz, & Völk (1988). Without coagulation to sizes  $\geq 1$  cm at 1 AU in the inner nebula, the timescale of planetesimal formation would exceed the lifetime of the nebula (Weidenschilling 1980).

Coagulation requires that two grains collide, with an impact gentle enough that they do not bounce apart, and then stick together due to van der Waals attraction (Weidenschilling 1980). The attractive force depends on the roughness and shape of the contact surface. The maximum collisional speed for coagulation depends on the grain size and the material's elastic properties and surface energy (Chokshi et al. 1993; Dahneke 1971). Ferromagnetism may sometimes promote coagulation (Nuth et al. 1994), and so may bipolar electric charging due to transient heating events (Horanyi & Goertz 1990).

Void-filled complex particles may be a common component of cosmic dust. This has been recognized in theories of coagu-

lation of randomly moving spheres, which predict that grains have a shape that is “fractal” (Meakin & Donn 1988) or “fluffy” (Chokshi et al. 1993). Void-filled particles have also been discovered in the laboratory, where experiments have shown that spongy structures grow easily, as discussed in §§ 3 and 5.3. In this paper, we present additional experimental evidence of spongy structures.

Despite the strength of the theoretical and experimental evidence supporting the existence of spongelike aggregates, they appear to be mentioned seldomly in the literature dealing with grain-size distributions for interstellar space and the protostellar nebula. One discussion, presented by Meakin & Donn (1988), proposed that a  $1 \text{ m s}^{-1}$  relative velocity, thought to be typical of grains in the primordial solar nebula, was conducive to forming fractal-like aggregates.

Carbonaceous materials and silicates probably constitute most grains in interstellar clouds. Carbon and SiC are thought to originate in the outflows of carbon stars, while silicates are produced by oxygen-rich stars (Bussoletti, Colangeli, & Orofino 1987; Zuckerman 1980; Gilman 1969). Based on meteorite analysis, it is thought that silicates are the chief non-icy solid ingredients in the presolar nebula that was the precursor of our own solar system.

Carbon is known to exist in space, but there is a controversy over its form. As evidence that carbon appears in graphite form, an absorption peak at 220 nm in the observed interstellar extinction spectra is often cited. Efforts to fit the observed spectra using scattering theory and models of the composition and size distributions have concluded that the peak is inexplicable except by including graphite as part of the grain mixture (Mathis, Rumpl, & Nordseick 1977). However, these arguments favoring graphite have been criticized as “highly speculative” by Czyzak, Hirth, & Tabak (1982). They proposed that the scattering parameters assumed in fitting the extinction peak are not well established by experiment or theory, that graphite has never been known to form spherical particles as postulated in these models, and that the high pressures and other thermodynamic conditions required for graphite crystal formation are not present in stellar outflows. Proponents of this view have argued that carbon is likely to appear in forms ranging from purely amorphous to polycrystalline, rather than graphite (Bussoletti et al. 1987). More recently, analysis of carbon grains extracted from meteorites, and claimed to be of interstellar origin, lends support to theories centering on graphite, because their microstructure often includes regions of mostly graphitized carbon (Bernatowicz et al. 1991).

### 3. PREVIOUS GRAIN SYNTHESIS EXPERIMENTS

The controversy over the form of carbon in space is just one example of a problem that could be clarified by laboratory experiments. Laboratory simulations also can provide data needed to interpret spectroscopic observations of scattering, extinction and emission from cosmic dust clouds. In fact, there are many problems in astrophysics that require a knowledge of the microscopic structure of dust grains and the microscopic processes that take place upon them, and they all can benefit from data supplied by experiments with cosmic dust analogs.

A method of synthesizing suitable dust grains is an essential part of these laboratory studies. Simply making a powder from a solid sample, by grinding or hammering, is unsuitable because it yields unrealistic shapes, like a corn flake. Instead, most experiments have grown grains by evaporation from a

solid sample, followed by condensation in the gas phase. This involves heating a solid target, by an arc discharge, oven, or a powerful laser (Nuth & Donn 1982; Capozzi, Flesia, & Minafra 1987; Stephens 1987; Iijima 1987a, b).

Spectroscopic data has been the goal of many experiments with cosmic grain analogs. Several experiments have reported IR absorption and UV extinction measurements for laboratory-synthesized grains, made of materials such as iron, carbon, silicon, silicon carbide, olivine, and  $\text{SiO}_2$  (Lefèvre 1970; Huffman 1975; Capozzi et al. 1987; Stephens 1987; Nuth et al. 1982, 1987). Capozzi et al. (1987) prepared samples of amorphous carbon dust with a spongy structure using an arc discharge between two amorphous carbon electrodes in an argon atmosphere, and they measured the UV extinction spectra. Stephens (1987) prepared silicate and carbon dust by vaporizing a solid target with a laser, and measured scattering intensities as a function of angle and wavelength. Additional spectroscopic experiments have been reviewed by Czyzak et al. (1982).

In addition to spectroscopy, laboratory studies have proven useful for characterizing grain growth processes. Coagulation has been the focus of several laboratory studies, although these are few in number and far from exhaustive. Lefèvre (1970) formed chains of  $0.1 \mu\text{m}$  size silica spheres by striking an arc in air. Onaka, Nakada, & Kamijo (1979) investigated the clustering of fine silicon particles by mutual thermal collisions. These fine particles were prepared in an argon gas atmosphere by an evaporation technique. Coagulation of silicon spheres was also observed by Iijima (1987a, b), who used an arc to produce a vapor. Nuth et al. (1994) produced very small iron grains in a low pressure hydrogen atmosphere in the presence of a magnetic field. These smokes became permanently magnetized, enhancing the coagulation rate enormously.

#### 4. NEW GRAIN SYNTHESIS TECHNIQUE

##### 4.1. Plasma Method of Synthesis

Evaporation methods of grain synthesis have certain limitations. A high temperature is required, and this has a great effect on the grain morphology. Grains are generated with specific size distributions that may be difficult to control. The movement of the particles themselves is also uncontrolled. Particles may grow as aggregates when that is not desired, yielding optical properties that can differ markedly from the properties of isolated spheres. The variety of materials that can be used is limited because the solid must evaporate at a reasonable temperature and pressure. Composite materials are difficult to synthesize, because the elemental constituents of alloys evaporate independently, at rates proportional to their respective vapor pressures.

As an alternative to evaporation schemes, we use here a new method of grain synthesis. A weakly ionized plasma is employed for three purposes. First, it produces ions that sputter a solid target, yielding an atomic flux of the desired material. This flux can collect on grains, making them grow by accretion. Second, it charges the grains so that they all repel one another, offering some control over coagulation by inhibiting it. Third, the plasma provides a controlled electrostatic levitation, suspending the grains for a long time in the region where they grow. When the plasma is switched off, the levitation ceases and grains fall to a surface. Many of them land on an electrode, which we insert into a scanning electron microscope to image the grains.

Sputtering is attractive for grain synthesis because it can produce an atomic vapor from a wider variety of solid materials, and at a lower temperature, compared to evaporation methods. Refractory materials can be sputtered easily, and the elemental constituents of an alloy target are sputtered at almost identical rates.

The sputtering process begins with ions that are extracted from the plasma. These are accelerated and strike a solid target, at normal incidence with an energy of several hundred electron volts. This sputters the target, ejecting atoms from the target surface into the surrounding environment. Details about the energy of the sputtered atoms are presented in Appendix A. Sputtered atoms can nucleate and form a grain, or they can stick to a grain that already exists. The latter process, grain growth by accretion of sputtered atoms, is sketched in Figure 2.

The target material determines the grain composition. Here, we used graphite targets to grow carbon grains, which are not necessarily in graphite form. Carbon is of interest because it is believed that about half of interstellar dust is in various forms of carbon-bearing components, while the rest is made of silicates. Our experimental method may be useful for synthesizing silicate grains, by using a composite target and adding oxygen to the process gas to increase its concentration in the grains to the desired level.

We briefly summarize the method below. A further explanation of our method is presented in another paper (Praburam & Goree 1994) and in the Appendix B, where we offer additional details not found elsewhere.

##### 4.2. Gas and Grains

To synthesize dust, we use a weakly ionized gas, in the form of a glow-discharge plasma. The discharge is operated at room temperature, and it can be sustained for hours. During this time, grains are electrostatically suspended a few millimeters above a sputtering target. They cannot move away from the growth region because electric fields trap them there. In this location, they are constantly exposed to the flux of sputtered atoms.

The discharge is struck by applying a radio-frequency (hereafter RF) high voltage across two parallel electrodes. A sketch of the apparatus is shown elsewhere (Praburam & Goree 1994). The upper electrode is powered, while the lower one is grounded. Argon at a pressure of less than 1 mBar was used in the experiment reported here. Argon was chosen because its ions provide a high sputtering yield, and the gas is inert and thus unlikely to be incorporated in the grains at concentrations above 2%. Other gases could be used in this method, if desired. The plasma is charge-neutral, except at the boundary between the plasma and a surface, where an electric sheath develops, as sketched in Figure 2. The sheath develops to prevent electrons from escaping more rapidly than ions. It also expels ions from the plasma and accelerates them toward the electrode surface, causing sputtering. Generally the electrode is covered with a target made of a desired material, in our case graphite, and the sputtered atoms come from that target.

The gas conditions we used in the laboratory are similar to the presolar nebula at 1 AU. The gas number density is the same ( $10^{15} \text{ cm}^{-3}$  at a pressure of  $1.33 \times 10^{-4}$  bar), and the gas temperatures are also comparable, with  $T = 300\text{--}600$  K in the laboratory and  $T = 600$  K at 1 AU in the presolar nebula (Weidenschilling 1980). The grain size also can be matched. The fractional ionization in our discharge ( $\approx 10^{-6}$ ) is compa-

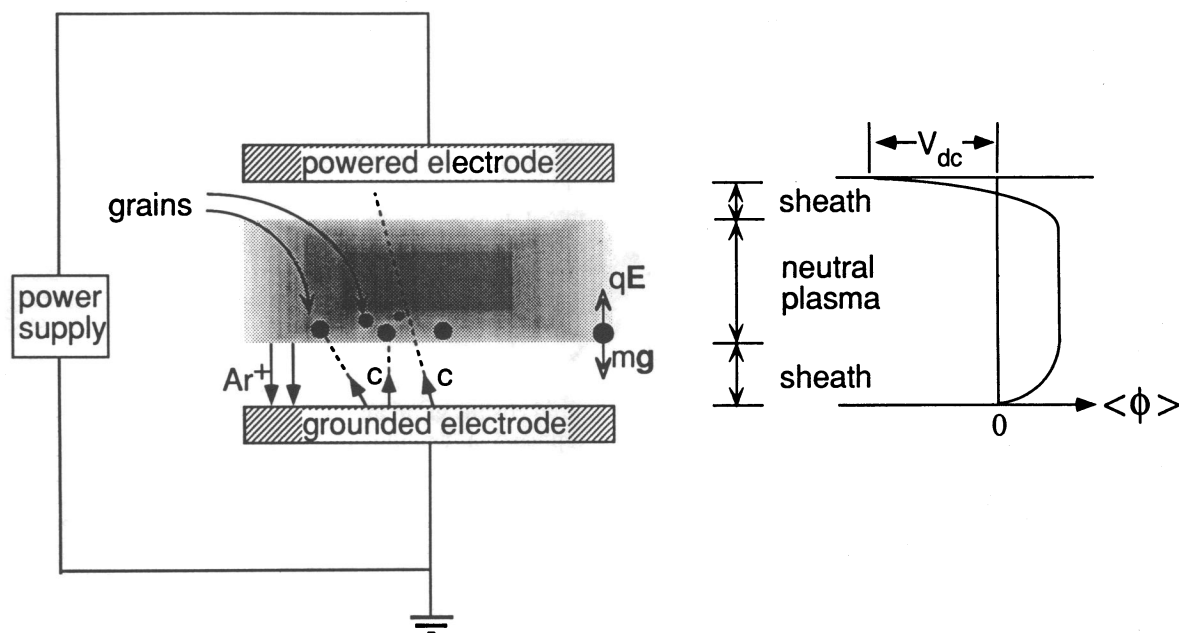


FIG. 2.—Sketch of the grain synthesis process. Grains are electrically suspended in the plasma. Ions are extracted from the plasma and accelerated through the sheaths at the electrode surfaces. Atoms sputtered from the surface due to ion bombardment are collected by grains so that they grow by accretion. Also shown is the electric potential profile between the electrodes, which provides the electrostatic levitation of negatively charged grains.

rable to that of the presolar nebula at 0.5 AU, but much higher than the  $10^{-13}$  ionization estimated at 1–3 AU (Stepinski 1992). The ionization fraction is also comparable to that in dense molecular clouds (Smith 1992; Norman & Heyvaerts 1985). In the experiment, the electron temperature is typically 10,000–30,000 K, as required to sustain the discharge and levitate the grains.

Grains are levitated and trapped in a localized region of the plasma. The levitation is provided by an upward electric field, due to a downward electrical field and the sheath and a negative charge on the grains. The grain is charged by absorbing electrons and ions, and the polarity is negative because electrons have a higher thermal velocity than ions (Goertz 1989). Grains are levitated at an equilibrium height where the electric force is balanced by the downward forces of gravity and ion drag. This equilibrium height varies with the charge-to-mass ratio, which decreases with grain size. For this reason, particles are stratified by size, with smaller grains suspended in layers above the larger grains. While the plasma is on, particles cannot escape the trap region, unless they grow so heavy that they fall of the lower electrode. When the plasma is switched off, the levitation ceases. Many of the particles collect on the lower electrode, which we remove for microscopic imaging.

#### 4.3. Procedure and Growth Conditions

The first step in our procedure was to use a scanning electron microscope (SEM) to image a fresh target, to verify that it was free of particles. Then we installed it in the apparatus and operated the plasma for minutes to hours, while using laser light scattering to monitor the spatial profile of the dust clouds. The plasma was then extinguished, causing the grains to fall. Finally, we removed the lower target without touching the grains, and inserted it again into the SEM, where the electron beam voltage was 0.7–10 keV. It was necessary to operate the SEM at 10 keV to resolve grains smaller than 300 nm. Otherwise we avoided using a beam energy greater than 5 keV, because energies above that level can alter the particle's surface

texture, making it smoother. The SEM never altered the particle size or coagulation state, regardless of the beam energy.

During the plasma operation, grains grew to a detectable size within the first few minutes. They were suspended in a thin cloud above the lower electrode, near the plasma-sheath boundary. This was revealed by the light scattering monitor and by simple visual observation. Figure 3 shows the scattered light signal as a function position, for a plasma operated at a pressure of  $5.5 \times 10^{-4}$  bar and a power density of 1–8 W

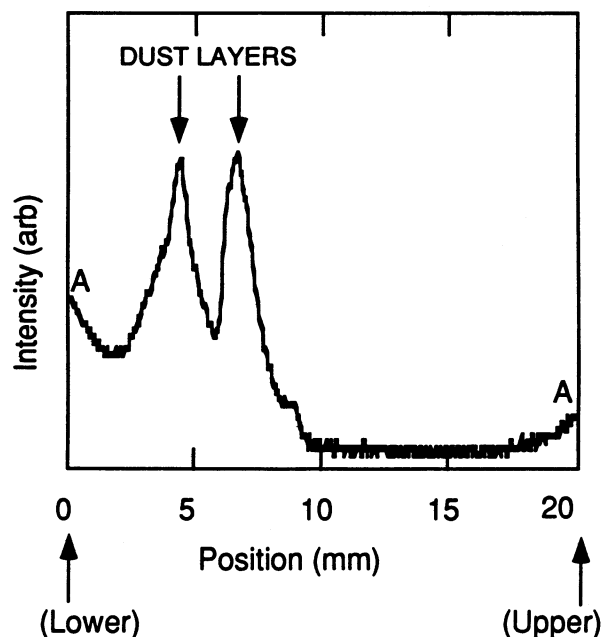


FIG. 3.—Spatial and temporal distribution of the grains levitated within the discharge. “Position” refers to height above the lower electrode. The laser scattering signal shown here increases with grain number density and size. Grains are concentrated in a few thin layers, levitated a few millimeters above the lower electrode. Features A are artifacts of scattered light from electrodes.

$\text{cm}^{-2}$ . The dust cloud was observed in the interelectrode region, where it was divided into stratified layers, separated according to grain sizes. The largest grains were seen levitated in the bottom-most layer.

Our emphasis in this paper is the study of the subsequent growth by accretion and coagulation, not the initial nucleation. In general, the nucleus could be homogeneous carbon or foreign material. For two reasons, we believe that our grains did not grow from foreign material. First, our grain growth results were repeatable after several months. Second, the signal from the laser-scattering monitor was always zero during the first few seconds after the plasma was ignited, and then increased gradually as grains grew.

The temperature of the surface of our grains during the growth process was 300–600 K. This value is based on particle temperature measurements reported by Daugherty & Graves (1993). They used a similar apparatus and similar experimental conditions, including the same gas pressure and RF power. The glow from a luminescent powder seeded into the plasma was measured, yielding the grain temperature. Their result, between 300 and 600 K, is reasonable because the grains will tend to thermalize with the gas, which is either at room temperature or slightly hotter due to heating by the plasma.

## 5. RESULTS

Several experiments were carried out to observe the morphology and growth processes of carbon grains. Initially, uncoagulated nanometer-size particles formed as individual spheres. This observation is consistent with growth by accretion. As time passed, grains continued to grow not only by accretion, but also by coagulation. In the early stages of coagulation, grains consisted of two or three small spheroids joined together. Then, as they were exposed for a longer time in the plasma, further collisions led to dozens of spheroids stuck together. Meanwhile, growth by accretion continued, even after the onset of coagulation. The results from these experiments are presented below, organized into sections according to the kind of morphology that was observed.

### 5.1. Spherical Grains Resembling a Cauliflower

Figure 4 (Plate 20) is an electron micrograph of carbon grains that grew during 420 minutes of plasma operation. These grains fell on the lower electrode. Note the spheroidal shape of the particles and the way that they are stuck together in a coagulated structure.

Spheroidal grains were often found to have a roughened surface resembling a cauliflower. This shape, which is evident in Figure 4, is not peculiar to our experiment. Other investigators with similar apparatus have reported growing cauliflower-shaped grains (Selwyn, Singh, & Bennet 1989; Ganguly et al. 1993). Figure 5 (Plate 21) shows the internal microstructure of a carbon grain collected by Ganguly et al. (1993), revealing that the particle is composed of columns radiating from the center. Each bump on the cauliflower surface is the head of a radial column. The columnar microstructure of grains grown by accretion was first reported by Selwyn et al. (1989), who synthesized grains that were uncoagulated and highly spherical.

This shape, a spheroidal cauliflower with an internal microstructure of radial columns, is probably very common for grains grown by accretion at a temperature well below the melting point. The surface temperature determines how easily an adsorbed atom can move about, and this helps determine

the microstructure of the surface as it grows. Much of what is known about the columnar microstructure and its temperature dependence comes from experiments done not with small particles, but with thin films of metal grown on planar substrates. The only difference between the surfaces of small particles and thin films is their geometry; a particle grows in columns radiating outward from a small core, while a planar thin film grows in columns standing parallel and shoulder-to-shoulder upon a planar surface. Experiments have shown that a thin film develops a columnar microstructure during its growth, if the surface is cooler than one-half or one-third the melting point of the sputtered material (Ross & Messier 1981; Hoffman & McCune 1990).

For comparison, we note that experimenters who synthesized cosmic grain analogs by evaporation methods have never reported a cauliflower shaped particle, to our knowledge. Instead, their grains often appear to be smooth-surfaced orbs. (Lefèvre 1970; Iijima 1987a, b). Although those experimenters did not report the temperature of their grains during the growth process, we assume that they were much hotter than the 300–600 K temperature of ours. This difference in grain temperature is an important distinction between the evaporation and sputtering methods of grain synthesis.

Spectroscopists may find it useful to know that the microstructure of the grain is sensitive to the temperature during growth. The microstructure is likely to affect the refractive index, which is an important parameter for interpreting spectroscopic observations of interstellar dust.

Grains shown in Figure 4 have a wide distribution of sizes, ranging from 10 nm to less than 1  $\mu\text{m}$ . This distribution is due to constant sputtering and grain growth during 420 minutes of discharge operation. We presume that the smaller grains are younger than the larger ones. At any time during the discharge, grains can begin growing from the sputtered flux. They fall to the electrode when the plasma is turned off, although some fall sooner, if they become massive enough that they can no longer be levitated.

### 5.2. Coagulation

Coagulated particles, consisting of several spheroids stuck together, were observed under some growth conditions. A typical example of coagulated grains is shown in Figure 6 (Plate 22), which was prepared with a long plasma exposure of 150 minutes.

The temporal development of grain growth and coagulation is revealed in Figures 7–10 (Plates 23–28). For this sequence, grains were grown during runs of 10, 20, 40, and 420 minutes, all with identical conditions. These figures show that as time passes, particles grow larger in diameter, and they are more likely to be coagulated. The number of spheroids per coagulated grain also increases with time. These results are reviewed below and summarized in Table 1.

After 10 minutes (Figs. 7a–7b) there were many spheroids of the same size, 100–150 nm, and very few were coagulated. Growth by accretion of atoms from the gas phase is expected to lead to individual spheroidal particles, like these. What might be surprising is the bumpy shape resembling a raspberry. Each bump on the surface is thought to be the head of a radial column, in its early stages of growth. After further growth it will lead to a cauliflower shape.

After 20 minutes (Fig. 8) the grains were 300–400 nm spheroids. A few were coagulated into structures of at most 10 grains. At this stage, growth is by accretion and coagulation,

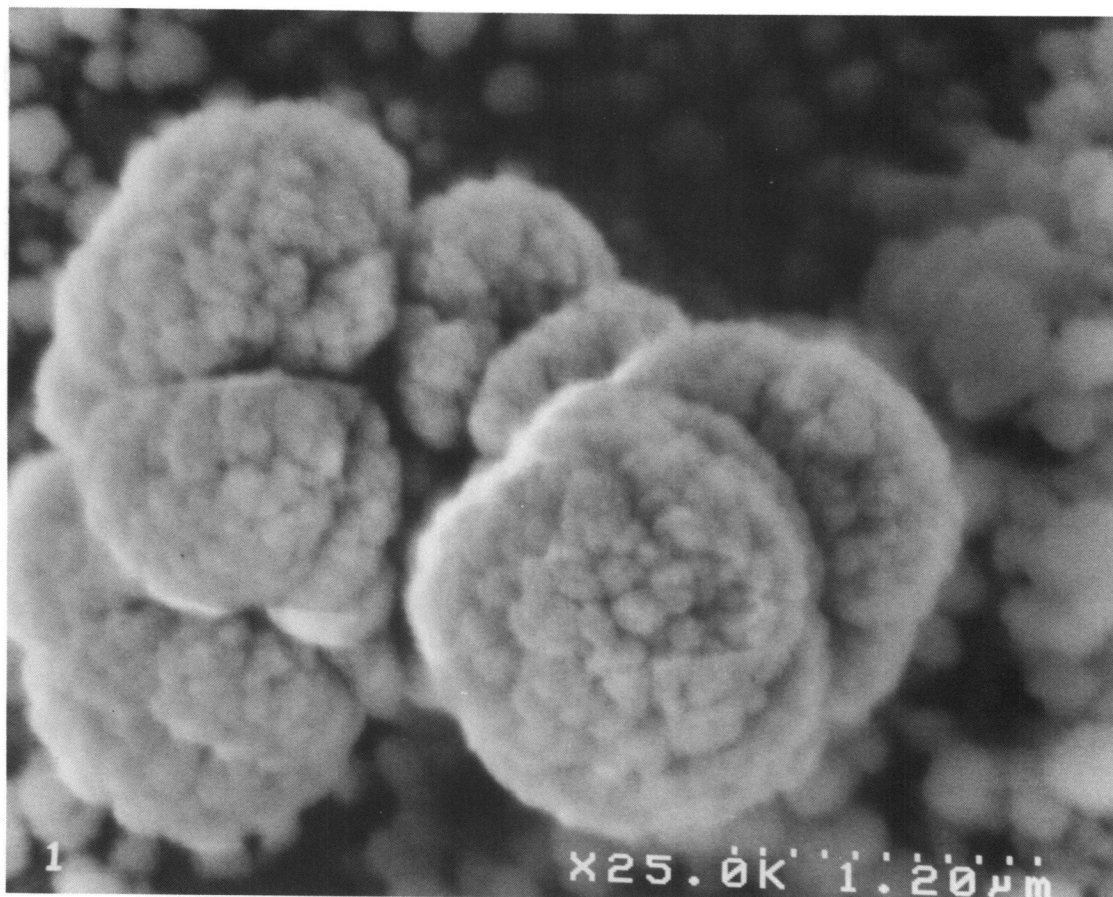


FIG. 4.—Electron micrograph of carbon grains grown after 420 minutes exposure. The grains have a wide size distribution and a cauliflower-like surface texture. Note the larger grains that have stuck together, forming a coagulated string. The calibration bar (a series of tick marks) of length  $1.2 \mu\text{m}$  indicates the size. The plasma was operated at  $5.5 \times 10^{-4}$  bar argon pressure and 120 W RF power.

PRABURAM & GOREE (see 441, 834)

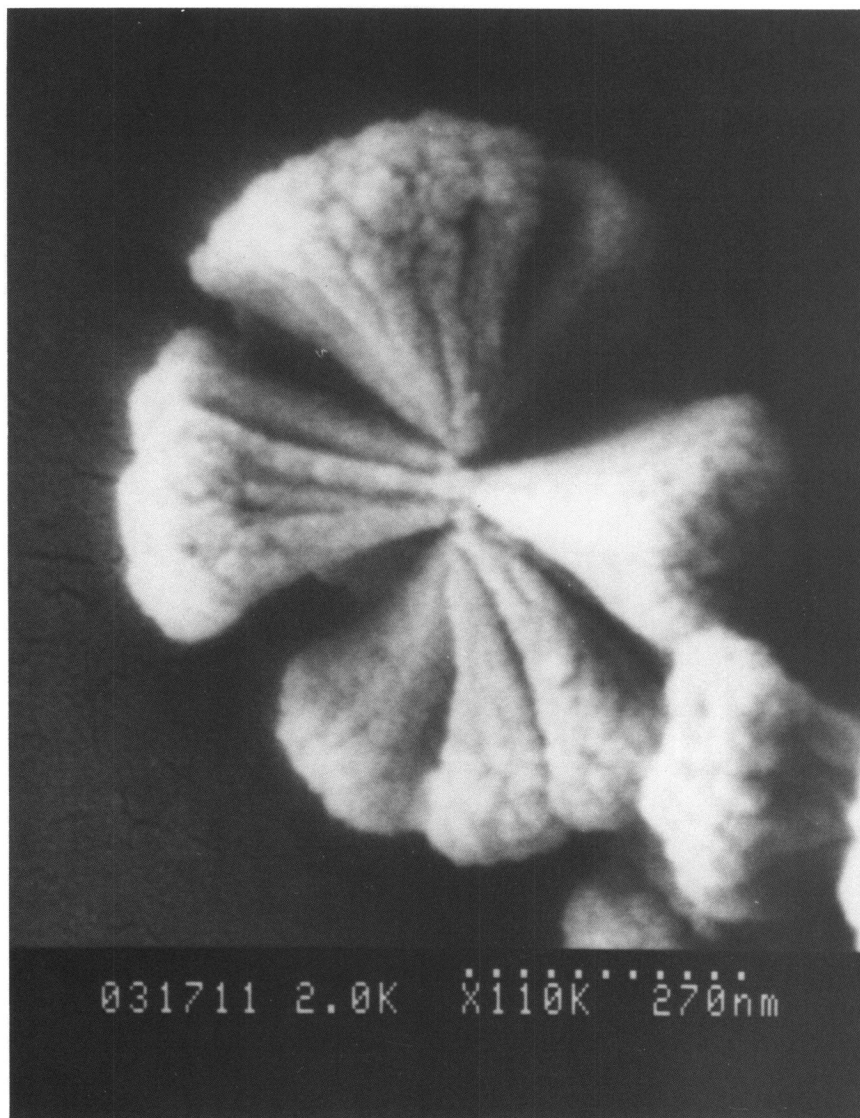


FIG. 5.—Carbon grain collected by Ganguly et al. (1993) in an experiment similar to ours. This grain was fractured, revealing the internal microstructure of columns radiating from the center. (Reprinted from Ganguly et al. 1993.)

PRABURAM & GOREE (see 441, 834)



FIG. 6.—SEM images of carbon grains collected after 150 minutes of plasma exposure. The discharge was operated at  $5.5 \times 10^{-4}$  bar argon pressure and 110 W RF power. Note the coagulated grains and the neck formed between them. The beam voltage of 10 keV used in the SEM for this and some other figures altered the surface texture of the grains, smoothing them so that they do not resemble a cauliflower.

PRABURAM & GOREE (see 441, 834)



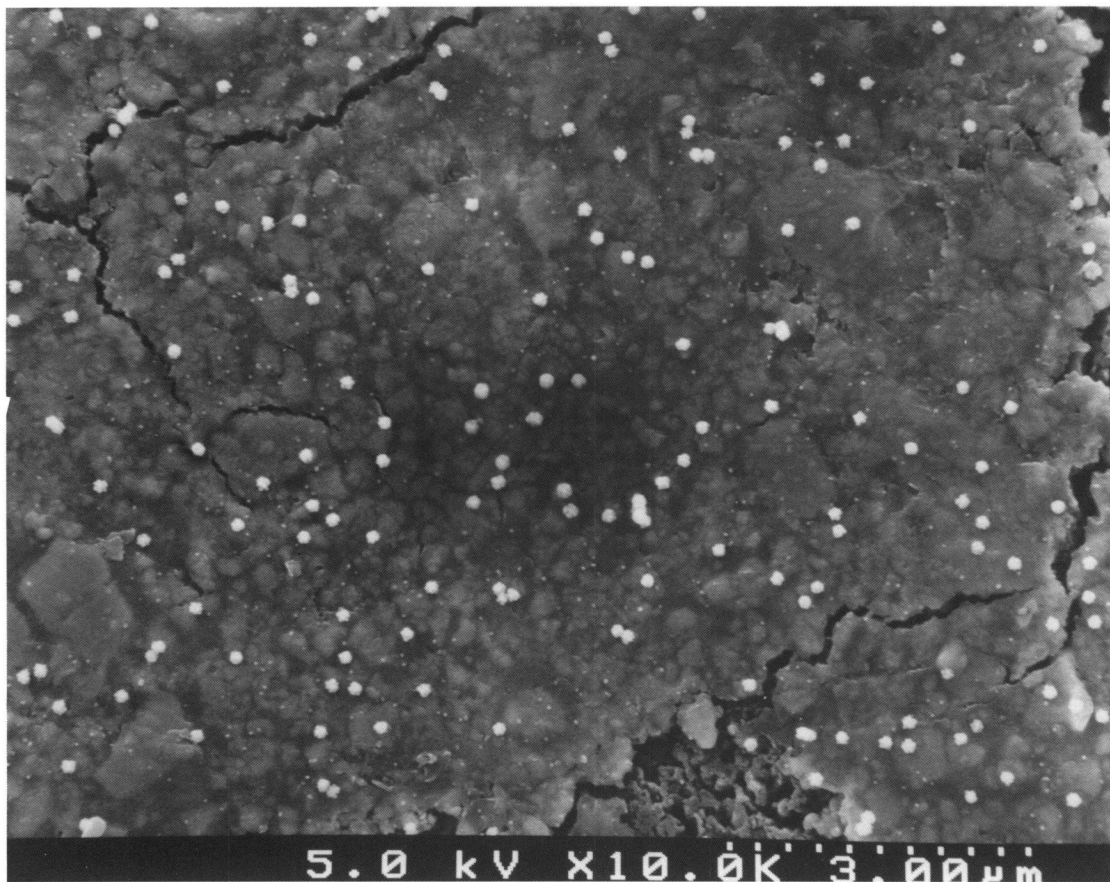


FIG. 7a

FIG. 7.—Carbon grains collected after 10 minutes. Figs. 8–10 continue this time sequence, all using the same discharge conditions as for Fig. 4. The particles are of 100–150 nm, have a uniform size distribution and are uncoagulated. The magnification is 6 times higher in (b) than in (a).

PRABURAM & GOREE (see 441, 834)

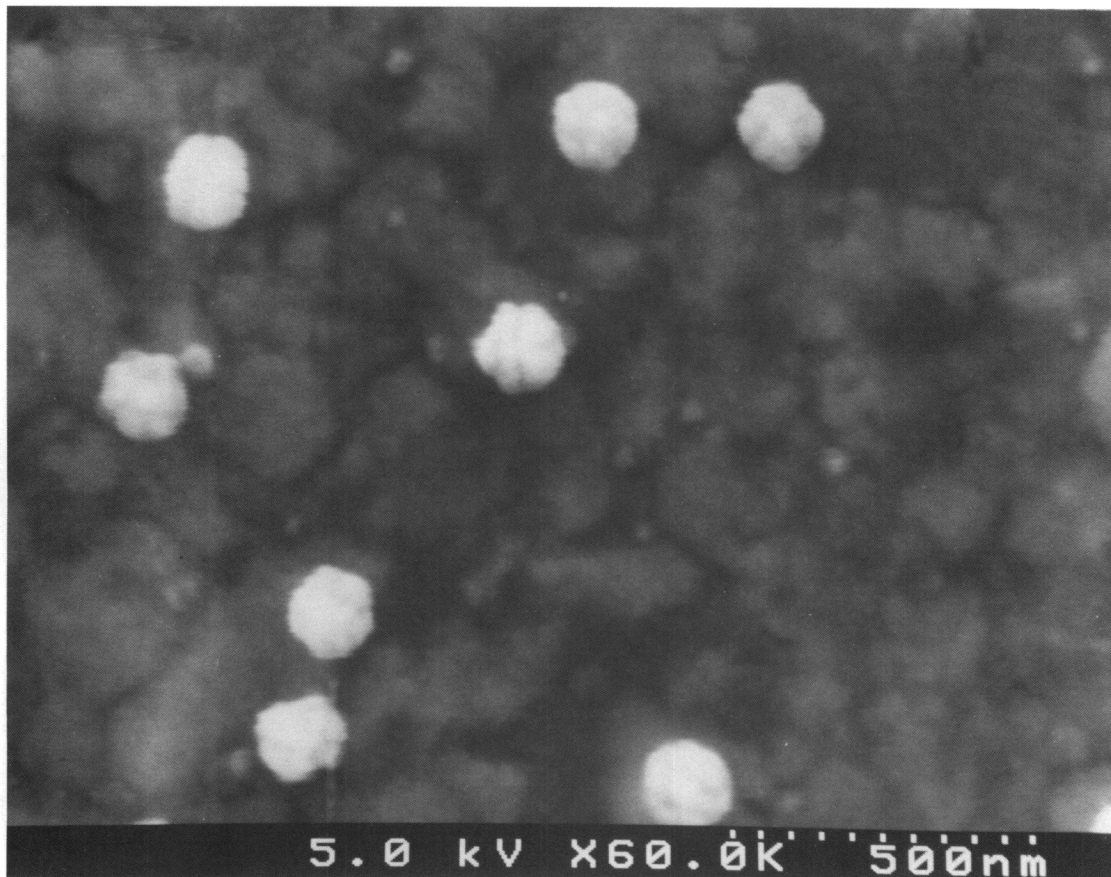


FIG. 7b

PRABURAM & GOREE (see 441, 834)

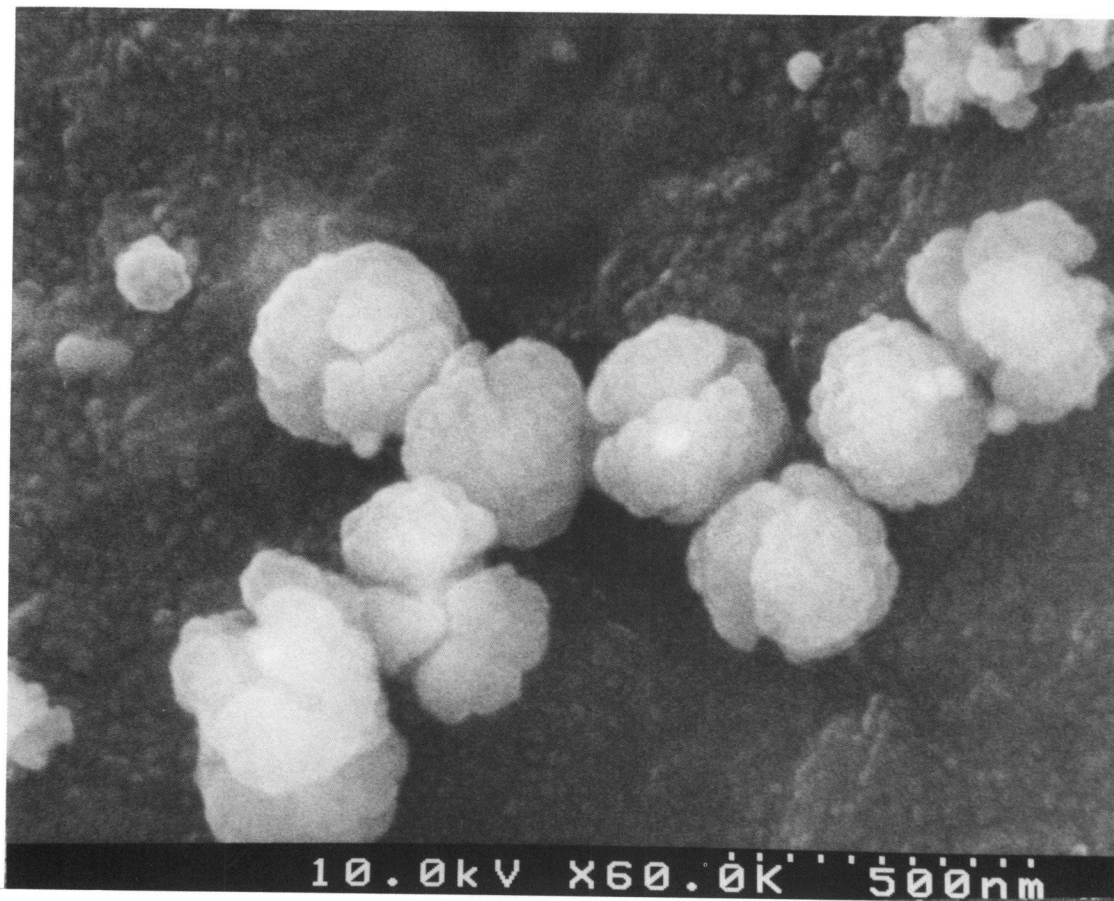


FIG. 8.—Carbon grain collected after 20 minutes. Note the particles that appear to have stuck together. The SEM beam voltage of 10 keV altered the surface roughness in this figure.

PRABURAM & GOREE (see 441, 834)

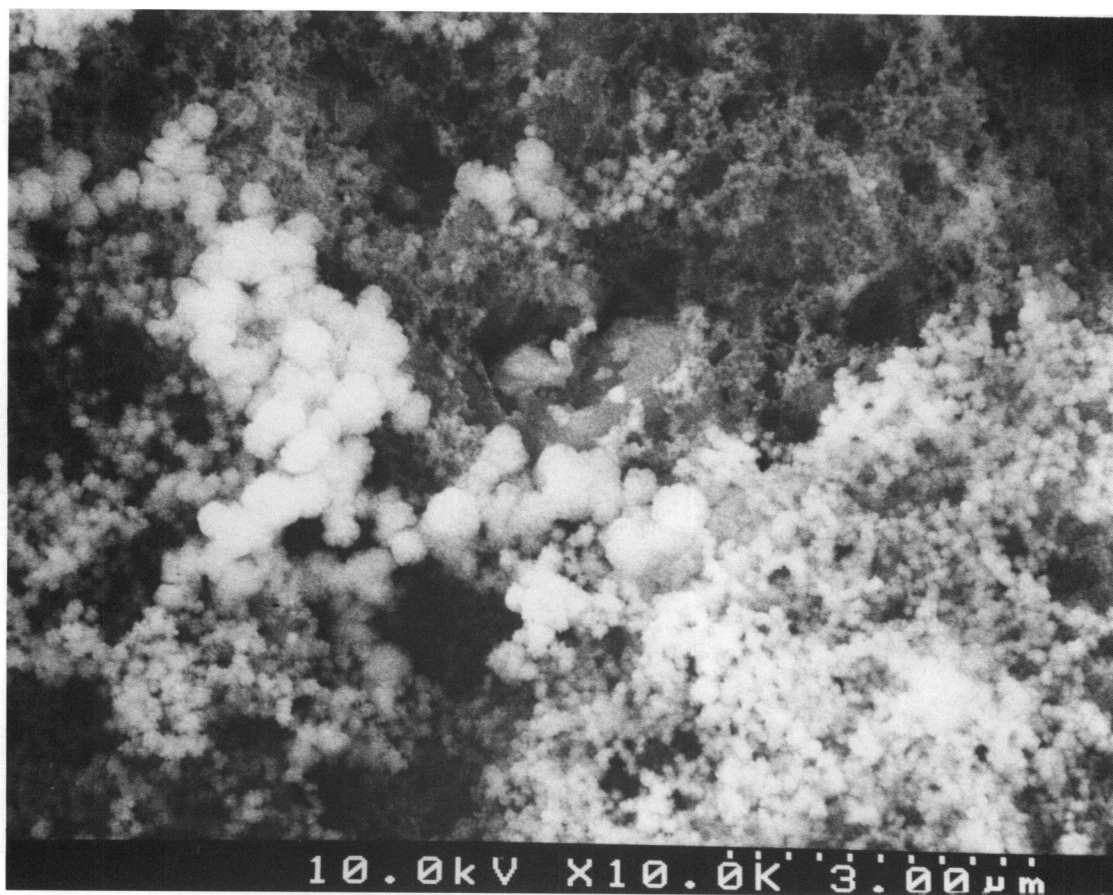


FIG. 9a

FIG. 9.—Carbon grains collected after 40 minutes. The particles have a wide size distribution. Note the coagulated structure of larger grains, and the spongy structure of smaller nanometer scale grains, which are too small to analyse using the SEM. In our experiment, spheroids tend to coagulate with other spheroids of approximately the same diameter. The magnification is 6 times higher in (b) than in (a).

PRABURAM & GOREE (see 441, 834)

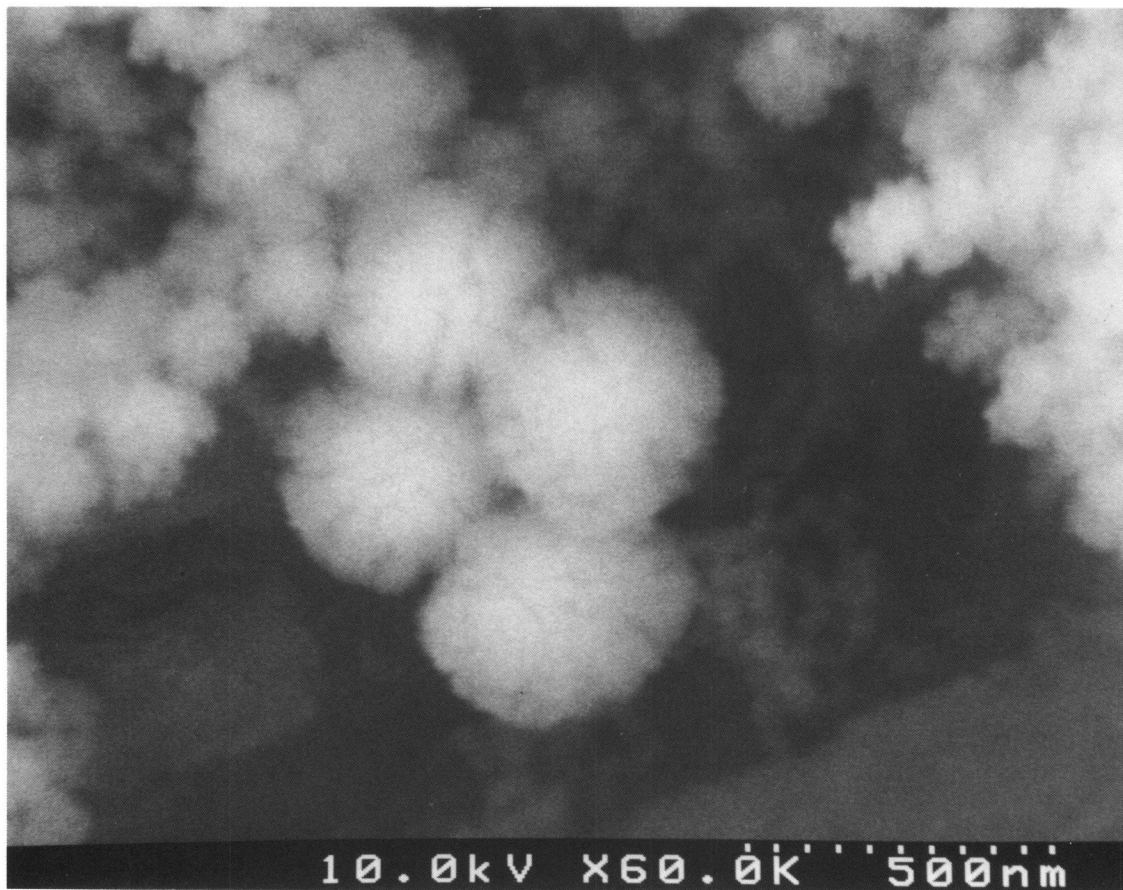


FIG. 9b

PRABURAM & GOREE (see 441, 834)

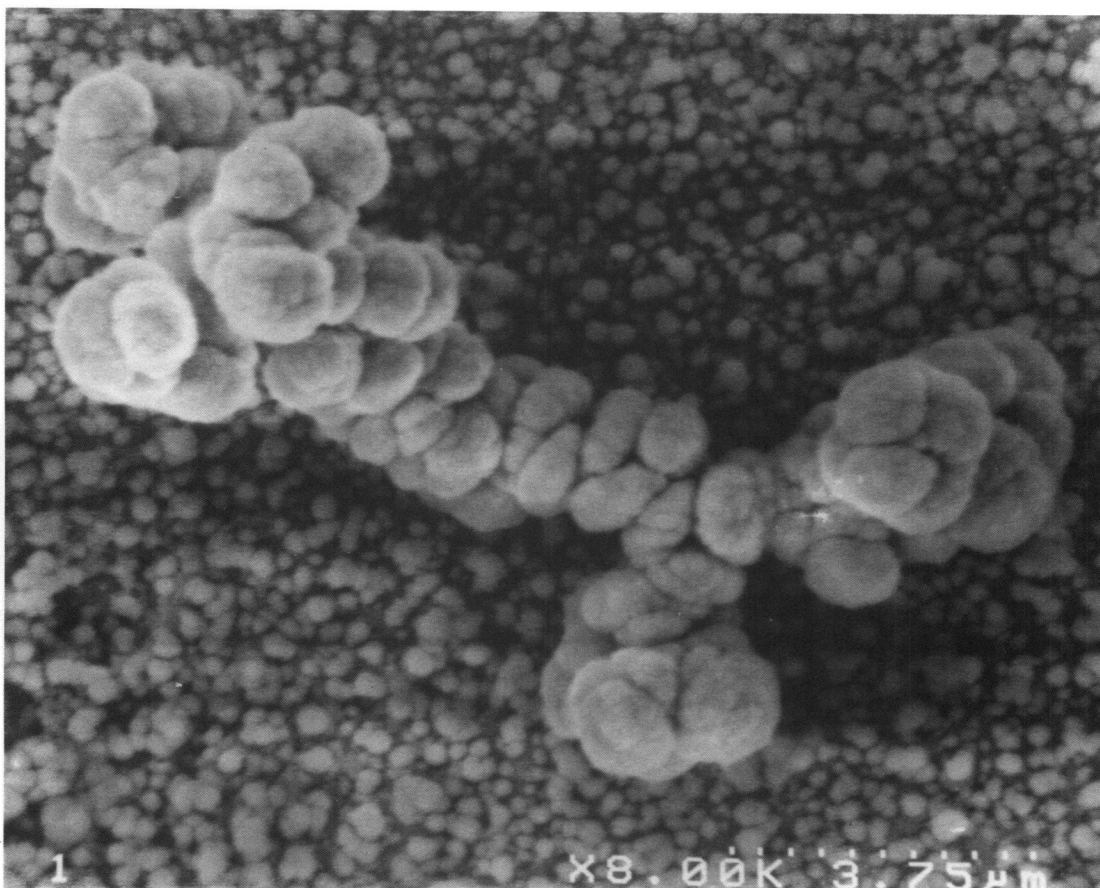


FIG. 10.—Carbon grains collected after 420 minutes. The spheroids have a cauliflower-like surface structure. Note the particles of  $1\ \mu\text{m}$  size that have stuck together, forming a coagulated string. The flatness of the spheroids indicates further growth by accretion following the coagulation.

PRABURAM & GOREE (see 441, 834)

TABLE 1  
RESULTS FROM A SERIES OF RUNS FOR VARIOUS EXPOSURE TIMES<sup>a</sup>

Time (minutes)	Figure Number	Spheroid Diameter (nm)	Coagulation	Number of Grains in a Coagulated Structure	Percent of Grains Coagulated
10 .....	7a-7b	< 100	No	...	0
		100-150	Yes	< 4	< 5
20 .....	8	< 100	Yes	< 10	> 20
		100-400	Yes	< 10	> 50
40 .....	9a-9b	< 50	Yes	Spongy	50
		50-400	Yes	> 10	< 50
		400-600	Yes	> 10	≥ 50
420 .....	10	< 50	Yes	Spongy	50
		50-300	Yes	< 10	< 50
		300-1.5 μm	Yes	> 10	≥ 50

<sup>a</sup> These results reveal the temporal development of grain growth. As time passes, spheroids grow larger in diameter by accretion, and are more likely to be found in a coagulated structure. Since spheroids developed a distribution of particle sizes, the observations of coagulation listed here are organized according to the size of the spheroids in a coagulated structure. These observations are based on several SEM images, including the figures.

with accretion dominating. (For this image, the SEM beam voltage was 10 keV, high enough to alter the surface texture of the grains in Fig. 8; this is the reason that they do not look like cauliflowers.)

After 40 minutes (Figs. 9a-9b) the grains have a wide distribution of sizes, from a few nanometers to 600 nm, and a larger fraction are coagulated. We presume that the smaller grains are younger than the large ones. The largest feature in Figure 9a is a coagulated structure of 400-600 nm spheroids.

After a much longer exposure of 420 minutes, we observed a few large string-shaped clusters of micron-size grains as shown in Figure 10. The grains within these clusters are flatter than the spheroids found for shorter exposures. The flattened appearance is attributable to further growth by accretion, after coagulation. After coagulation, the spacing of spheroids in a structure is fixed, and atoms that stick to them can only increase their girth.

The morphology of our coagulated grains is revealing. Some images, such as Figure 6, reveal a clearly identifiable "neck" joining two spheroids. Such a neck is expected to form after two grains collide and dissipate their kinetic energy. It develops due to the attractive force, which deforms the particles to make a substantial contact area. (Choksi et al. 1993).

To validate our coagulation results, it is necessary to verify that the coagulation took place while the grains were suspended in the gas phase, and not afterward. To exclude the possibility of coagulating during *ex situ* handling after the plasma was turned off, we avoided disturbing them. The grains were left on the electrode just as they fell, and the entire electrode was transferred into the SEM. Another possibility that must be excluded is that isolated grains landed upon one another when they fell to the electrode, creating an agglomerate that never existed in the gas phase. We can dismiss this possibility by noting that the number of spheroids per agglomerate increases with exposure time and by verifying that the 3D arrangement of the spheroids in the coagulated structures does not resemble a heap. These observations are consistent with the coagulation taking place while suspended in the plasma, not on the electrode surface.

Coagulation requires enough relative velocity  $v$  for two grains to overcome the electric repulsion (Simpson, Simon, & Williams 1979). This criterion is  $mv^2/4 > (q^2/4\pi\epsilon_0)/2a$ , for two

identical grains of charge  $q$ , mass  $m$ , and radius  $a$  (Horanyi & Goertz 1990). To use this, we need the charge, which could not be measured. We shall estimate  $q$  by assuming thermal electrons with a temperature of 30,000 K, typical for discharges of this type, and using a standard charging model (Cui & Goree 1994). For an isolated 1 μm grain, this yields  $q \approx -3100 e$ . A collision between a pair of these grains requires a relative velocity of 200 cm s<sup>-1</sup>. This collisional velocity is three orders of magnitude faster than the thermal velocity of 0.2 cm s<sup>-1</sup>, which one would expect if the grains are thermalized with the gas at  $T = 300$  K. To remedy this discrepancy, either the charge must be smaller, or it must be attractive, or the particle velocity must be higher.

While the charge might be smaller than we have estimated, this is by itself inadequate to explain the discrepancy. A reduction of the charge, due to electron depletion at high grain number densities (Havnes, Aanesen, & Melandsoe 1990), is less than one order of magnitude for the parameters for our experiment.

The possibility of attraction between oppositely charged grains can be dismissed. While it is true the grains in the pre-solar nebula and other cosmic dust plasmas can have either polarity (Horanyi & Goertz 1990), in our small discharge all the grains must be negative. If a grain were to develop a positive charge, it would be expelled immediately, rather than confined by the plasma's electric field, which points everywhere away from the plasma center.

Thus, a high particle velocity is the only remaining explanation. This led us to conduct an experiment that revealed a significant fraction of superthermal grains in our dusty plasma. In this test, we used a different apparatus, but with a similar configuration and size. It was equipped with a video camera and a macro lens to image grains in the plasma. An expanded He-Ne laser beam illuminated the dust cloud. We operated the discharge with similar parameters (55 Pa argon pressure and ≤ 30 W RF power). The grains were larger so that we could image them individually and measure their velocity. We used 20-40 μm aluminum oxide particles, which were seeded into the plasma. Using a video tape, frame-by-frame measurements of particle position yielded the velocity of individual grains. Several percent of the particles had superthermal velocities of 2-4 cm s<sup>-1</sup>, while most particles moved at a much lower

thermal velocity. The fraction of superthermal grains was found to increase with RF power. To extrapolate these results to the carbon-grain coagulation experiment, we assume that 1  $\mu\text{m}$  carbon grains will have the same kinetic energy as the larger aluminum oxide grains. Then, a 1  $\mu\text{m}$  carbon grain would have a velocity of 300–600  $\text{cm s}^{-1}$ , which is above the relative velocity of 200  $\text{cm s}^{-1}$  required for coagulation, as estimated above.

We found that achieving coagulation in our experiment required operating with a certain set of plasma parameters. These conditions were an argon pressure greater than 55 Pa and an RF power of 110 W. We tested many different settings for the power and pressure and not all of them led to coagulation.

### 5.3. Spongy Structure

Large spongy structures composed of nanometer-size particles were observed after 40 minutes of growth, under some plasma conditions. Figure 9 shows a typical void-filled spongy structure. The SEM revealed that this sponge covers not just the area shown in the image, but the entire electrode surface. Larger spheroids happen to rest upon this structure. The spongy structure apparently consists of individual particles, too small to image with the SEM, separated with many voids. These structures were often found when the discharge was operated at pressures greater than 55 Pa, the same conditions that also led to coagulation of larger spheroids, as described above.

Similar void-filled aggregates have been synthesized by other laboratory experimenters (Capozzi et al. 1987; Nuth et al. 1994). According to theory, these fluffy aggregates can form if the relative grain velocity is less than several meters per second (Meakin & Donn 1988; Donn 1987). Velocities in this range are estimated for micron size or smaller grains in the primordial solar nebula. Therefore, it has been postulated that “fractal particles” were present in the solar nebula (Meakin & Donn 1988).

### 5.4. Grains Resembling Interstellar and Interplanetary Particles

It is instructive to compare our laboratory-synthesized grains to actual cosmic grains. There are two candidates for comparison: embedded grains extracted from meteorites and chondritic grains collected by aircraft in the terrestrial stratosphere. In both cases, there is a striking resemblance to Figure 11 (Plate 29), which shows a grain synthesized in our experiment with the same pressure as before, but a reduced RF power of 55 W. Particles synthesized under these conditions do not resemble a cauliflower.

A carbon spherule extracted from the Murchison carbonaceous meteorite by Bernatowicz et al. (1991, their Fig. 1) has a lumpy spheroidal shape with a surface texture of rounded bumps. It closely resembles our grain in Figure 11. The Murchison spherule is thought to be an interstellar grain, and analysis showed that it contains carbon in various phases, including graphite.

Another striking similarity is the similar appearance of the grain in Figure 11 and a chondritic grain collected by Brownlee et al. in the terrestrial stratosphere. Large numbers of these micron-size particles have been collected using a U2 aircraft. (Brownlee, Rajan, & Tomandl 1977; Rajan et al. 1977). They are believed to be of interplanetary origin, perhaps from comets, and they appear to be aggregates of smaller particles. While they do not all look alike, at least one of them (Hill & Mendis 1979) resembles our grain in Figure 11.

## 6. SUMMARY

We used a new laboratory method to synthesize cosmic grain analogs at room temperature. A low-pressure plasma powered by a radio-frequency high voltage is used to sputter a target, producing a flux of atoms, which promotes grain growth by accretion. The grains are levitated and suspended in the plasma during several hours of plasma operation. During this time they can collide and grow by coagulation. The gas and particle conditions in the apparatus are similar to those hypothesized for the presolar nebula.

We grew carbon grains, which were usually spheroids. Under most experimental conditions they had a cauliflower-like surface and an internal microstructure of radial columns. This microstructure is probably common for grains grown by accretion at a temperature well below the melting point. Under other conditions, nonspherical grains were grown that did not resemble a cauliflower, but bore a close resemblance to both an interstellar graphite spherule and a chondritic grain collected in the terrestrial stratosphere.

We synthesized two kinds of agglomerated particles under certain experimental conditions. One kind was coagulated particles composed of spheroidal cauliflowers pressed together in string-shaped masses. These were joined by a neck at the point of contact. The longer they were exposed to the plasma, the larger the fraction that coagulated. Another kind of agglomerated particle was a large spongy structure. These void-filled masses consisted of nanoscale particles too small to detect using an SEM.

Coagulation of electrically charged grains requires a large interparticle velocity to overcome the repulsive potential. This velocity must be far higher than the thermal velocity at the neutral gas temperature. Thus, superthermal grains are thought to be responsible for coagulation in our experiments. Measurements of grains large enough to image individually indicate that a fraction have a superthermal velocity, consistent with our coagulation observations.

We thank B. Ganguly for helpful discussions and for permitting us to reprint his electron micrograph, J. D. Fix for helpful discussions, and T. Bernatowicz for providing us with his results. This work was supported by NASA Origins of the Solar System Program NAGW-3126, NASA NAG 8-292, and NSF ECS-92-15882.

## APPENDIX A

### ENERGY OF SPUTTERED ATOMS

Sputtering is the removal of atoms from a solid surface due to bombardment by energetic atoms or ions. The ejected atoms have energy and angular distributions that are functions of the ion's mass, energy, and angle of incidence. The number of target atoms sputtered per incident ion is called the sputtering yield, and this too is a function of the ion's angle of incidence (Zalm 1989;



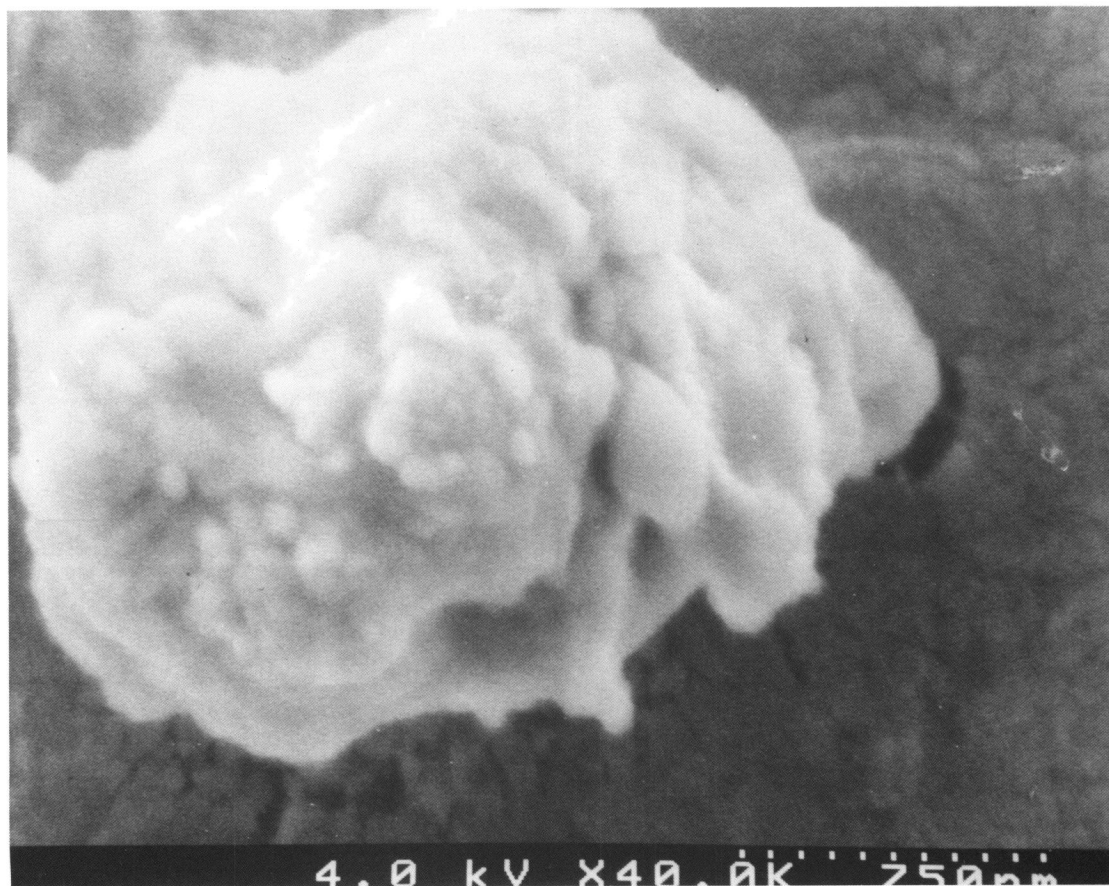


FIG. 11.—Carbon grain collected in our experiment, which looks like a carbon grain extracted from a meteorite (Bernatowicz et al. 1991) and like a chondritic aggregate grain collected by Brownlee and others (Hill & Mendis 1979). The plasma parameters were the same as before, except that the RF power was reduced.

PRABURAM & GOREE (see 441, 836)

Townsend, Kelley, & Hartley 1976). In our apparatus, a strong electric field concentrated in a thin sheath accelerates ions so that they strike the electrode at normal incidence.

By the time the sputtered atoms reach the grain-growing region in our apparatus, they are thermalized with the ambient gas, with  $T = 300\text{--}600$  K. They do not start that way, however. When they are ejected from the surface, they have much more energy. Their energy spectrum has a most probable energy of 2 eV, and due to an energetic tail, a mean of  $\sim 12$  eV (Eckstein 1987). The angular distribution is concentrated in the range from  $0^\circ$  to  $30^\circ$  (Zalm 1989).

Most of the excess energy in the sputtered flux is lost before it reaches the particle formation region, 4–7 mm from lower electrode and 13–16 mm from the upper electrode. This happens due to a few collisions with the neutral atoms in the gas. We can quantify the energy loss using the results of Meyer, Shuller, & Falco (1981). They computed the energy distribution of sputtered copper atoms as a function of the distance travelled through the argon gas. They used an argon pressure of  $1.33 \times 10^{-5}$  bar, which is  $\sim 40$  times lower than in our experiment. Accordingly, we scale the distances in their data downward by a factor of 40, assuming that the collision cross sections are the same for carbon and copper. Figure 12 shows how the sputtered atoms are thermalized after traveling  $\sim 5$  mm, which is far enough to reach the dust clouds. The atoms will also be isotropized by the collisions.

## APPENDIX B

### ADDITIONAL DETAILS OF APPARATUS

As sketched elsewhere (Fig. 1 of Praburam & Goree 1994), the setup is centered on a cylindrical aluminum vacuum vessel, fitted with windows for making optical measurements. In it are installed a pair of 6.2 cm diameter electrodes, which lie in a precise horizontal alignment so that the force of gravity is normal to the surface. Each is covered by a disk-shaped graphite target clamped to a stainless steel base. The upper electrode is water-cooled, since most of the  $\approx 100$  W of power is ultimately deposited there. We applied a 13.56 MHz radio-frequency voltage to the upper electrode by coupling the output of a power amplifier through an impedance matching network and a coupling capacitor to the electrode's vacuum feedthrough. Further details of our experimental apparatus are presented elsewhere (Praburam & Goree 1994). An alternate configuration was used by Ganguly et al. (1993); it was constructed of glass tubes rather than a metal vacuum vessel.

We used a turbopump, which like a molecular-drag pump prevents any oil contamination. However, these experiments are conducted at a relatively high pressure (a few tens of mbar), so one might avoid the expense of these pumps by using merely a mechanical pump with a trap to reduce oil backstreaming.

Experiments can be performed with or without gas flow. We found much less particle growth in our apparatus when we shut off the flow, but Ganguly et al. (1993) successfully operated their glass tube without any flow.

Besides the high frequency we used, the electrodes may be powered with audio frequency or DC voltages. Ganguly et al. (1993) used an audio frequency discharge with graphite electrodes to grow carbon grains. He performed the experiment without gas flow in a sealed glass discharge tube. To concentrate the plasma between the electrodes, it is necessary to isolate the electrode supports. At

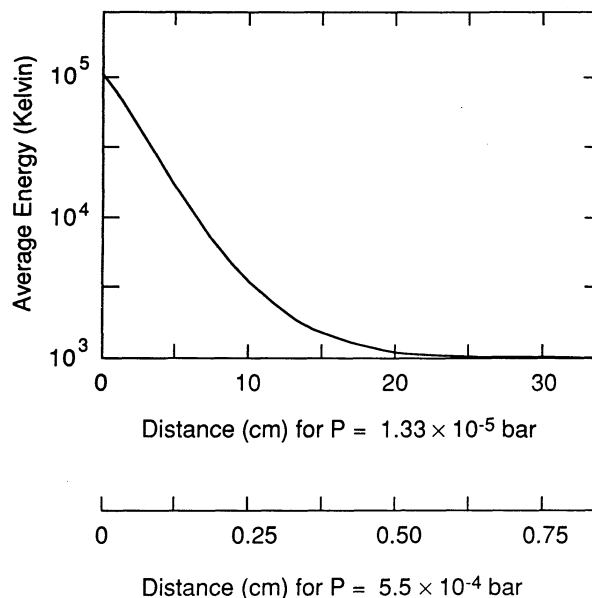


FIG. 12.—Average energy of sputtered atoms as a function of distance traveled from target. These data (Meyer et al. 1981) show how sputtered copper atoms are cooled by collisions with argon atoms, and become thermalized after traveling a distance of 20 cm through a gas with a pressure of  $1.33 \times 10^{-5}$  bar. For our experiment, the corresponding distance is 5 mm from our electrode, at an argon pressure of  $5.5 \times 10^{-4}$  bar, as shown on the lower scale. Energy is shown here in temperature units, kelvin.

low frequencies they can be covered by glass, while at 13.5 MHz a ground shield is required. Jellum & Graves (1990) used a DC discharge with aluminum electrodes to grow aluminum particles. Yet when we tested DC power in our apparatus, we found that it did not lead to the easy levitation that is typical of radio-frequency powered discharges. A further advantage of radio frequency power is that it allows the sputtering of nonconductive targets. We did not test audio frequency discharges using our setup.

It may be useful to know some conditions that prevail inside a typical glow discharge, regardless of how it is powered and whether there is gas flow. In glow discharges, the gas is weakly ionized, with an electron number density of typically  $10^{10} \text{ cm}^{-3}$ , compared to a neutral gas density of  $\sim 10^{15} \text{ cm}^{-3}$ . The ionization is sustained by electron impact on the neutral atoms or molecules. Electrons have a temperature of  $\sim 30,000 \text{ K}$ , while the ions are in equilibrium with the neutral gas. The gas temperature may be elevated slightly above room temperature due to the power applied to the discharge. These are the conditions in which the grains are found in our process.

## REFERENCES

- Bernatowicz, T. J., Amari, S., Zinner, E. K., & Lewis, R. S. 1991, *ApJ*, 373, L73  
 Brownlee, D. E., Rajain, R. S., & Tomandl, D. A. 1977, in *Comets, Asteroids, Meteorites—Interrelations, Evolution, and Origins*, ed. A. H. Delsemme (Toledo: Univ. Toledo), 137  
 Bussoletti, E., Colangeli, L., & Orofino, V. 1987, in *Experiments on Cosmic Dust Analogues*, ed. E. Bussoletti, C. Fusco, & G. Longo (Dordrecht: Kluwer), 63  
 Capozzi, V., Flesia, C., & Minafra, A. 1987, in *Experiments on Cosmic Dust Analogues*, ed. E. Bussoletti, C. Fusco, & G. Longo (Dordrecht: Kluwer), 153  
 Cassinelli, J. P. 1979, *ARA&R*, 17, 275  
 Chokshi, A., Tielens, A. G. G. M., & Hollenbach, D. 1993, *ApJ*, 407, 806  
 Cui, C., & Goree, J. 1994, *IEEE Trans. Plasma Sci.*, 22, 151  
 Czyzak, S., Hirth, J., & Tabak, R. 1982, *Vistas Astron.*, 25, 337  
 Dahneke, B. 1971, *J. Colloid Interface Sci.*, 37, 342  
 Daugherty, J. E., & Graves, D. B. 1993, *J. Vac. Sci. Technol. A*, 11, 1126  
 Donn, B. D. 1987, in *Experiments on Cosmic Dust Analogues*, ed. E. Bussoletti, C. Fusco, & G. Longo (Dordrecht: Kluwer), 43  
 Draine, B. T., & Salpeter, E. E. 1979, *ApJ*, 231, 438  
 Eckstein, W. 1987, *Nucl. Instrum. Methods*, B18, 344  
 Ganguly, B., Garscadden, A., Williams, J., & Haaland, P. 1993, *J. Vac. Sci. Technol. A*, 11, 1119  
 Gilman, R. C. 1969, *ApJ*, 155, L185  
 Goertz, C. K. 1989, *Rev. Geophys.*, 27, 271  
 Goree, J. 1994, *Plasma Sources Sci. Tech.*, 3, 400  
 Havnes, O., Aanesen, T., & Melandsø, F. 1990, *J. Geophys. Res.*, 95, A5, 6581  
 Hill, J. R., & Mendis, D. A. 1979, *Moon & Planets*, 21, 3  
 Hoffman, D. W., & McCune, R. C. 1990, in *Handbook of Plasma Processing Technology*, ed. S. M. Rossnagel, J. J. Cuomo, & W. D. Westwood (Park Ridge, NJ: Noyes), 483  
 Horanyi, M., & Goertz, C. K. 1990, *ApJ*, 361, 155  
 Huffman, D. R. 1975, *Ap&SS*, 34, 175  
 Iijima, S. 1987a, *Japanese J. Appl. Phys.*, 26, 357  
 ———. 1987b, *Japanese J. Appl. Phys.*, 26, 365  
 Jellum, G. M., & Graves, D. B. 1990, *J. Appl. Phys.*, 67, 6490  
 Johnson, R. E., & Lanzerotti, L. J. 1986, *Icarus*, 66, 619  
 Lattimer, J. M. 1982, in *Formation of Planetary Systems*, ed. A. Brahic (Toulouse: Cepadues-editions), 189  
 Lefèvre, J. 1970, *A&A*, 5, 37  
 Mathis, J., Rumpl, W., & Nordsieck, K. 1977, *ApJ*, 217, 425  
 Meakin, P., & Donn, B. 1988, *ApJ*, 329, L39  
 Meyer, K., Shuller, I. K., & Falco, C. M. 1981, *J. Appl. Phys.*, 52, 5803  
 Mizuno, H., Markiewicz, W. J., & Völk, H. J. 1988, *A&A*, 195, 183  
 Nishi, R., Nakano, T., & Umebayashi, T. 1991, *ApJ*, 368, 181  
 Norman, C., & Heyvaerts, J. 1985, *A&A*, 147, 247  
 Northrop, T. G., & Hill, J. R. 1983, *J. Geophys. Res.*, 88, 1  
 Nuth, J. A., III, Berg, O., Faris, J., & Wasilewski, P. 1994, *Icarus*, 107, 155  
 Nuth, J. A., & Donn, B. 1982, *J. Chem. Phys.*, 77, 2639  
 Nuth, J. A., Nelson, R. N., Moore, M., & Donn, B. 1987, in *Experiments on Cosmic Dust Analogues*, ed. E. Bussoletti, C. Fusco, & G. Longo (Dordrecht: Kluwer), 191  
 O'Dell, C. R., & Wen, Z. 1994, *ApJ*, 436, 194  
 Onaka, T., Nakada, Y., & Kamijo, F. 1979, *Ap&SS*, 6, 103  
 Praburam, G., & Goree, J. 1994, *J. Vac. Sci. Technol. A*, 12, in press  
 Rajan, R. S., Brownlee, D. E., Tomandl, D., Hodge, P. W., Farrar H., IV, & Britten, R. A. 1977, *Nature*, 267, 133  
 Ross, R. C., & Messier, R. 1981, *J. Appl. Phys.*, 52, 5329  
 Seab, C. G., & Shull, M. 1983, *ApJ*, 275, 652  
 Selwyn, G. S., Singh, J., & Bennett, R. S. 1989, *J. Vac. Sci. Technol. A*, 7, 2758  
 Simpson, I. C., Simons, S., & Williams, I. P. 1979, *Ap&SS*, 61, 65  
 Smith, D. 1992, *Plasma Phys. Controlled Fusion*, 34, 1817  
 Stephens, J. R. 1987, in *Experiments on Cosmic Dust Analogues*, ed. E. Bussoletti, C. Fusco, & G. Longo (Dordrecht: Kluwer), 245  
 Stepinski, T. F. 1992, *Icarus*, 97, 130  
 Thomas, H., Morfill, G. E., Demmel, V., Goree, J., Feuerbacher, B., & Möhlmann, D. 1994, *Phys. Rev. Lett.*, 73, 652  
 Townsend, P. D., Kelley, J. C., & Hartley, N. E. W. 1976, *Ion Implantation, Sputtering, and their Applications* (London: Academic)  
 Wehner, G. K., Kenknight, C., & Rosenberg, D. L. 1963, *Planet. Space Sci.*, 11, 885  
 Weidenschilling, S. J. 1980, *Icarus*, 44, 172  
 Weitz, D. A., & Oliveria, M. 1984, *Phys. Rev. Lett.*, 52, 1433  
 Wetherill, W. H. 1978, in *Protostars and Planets*, ed. T. Geherls (Tucson: Univ. of Arizona Press), 565  
 Woolf, N. J., & Ney, E. P. 1969, *ApJ*, 155, L181  
 Zalm, P. C. 1989, in *Handbook of Ion Beam Processing Technology*, ed. J. J. Cuomo et al. (Park Ridge, NJ: Noyes), 78  
 Zuckerman, B. 1980, *ARA&R*, 18, 263